

## COMMUNICATIONS

# Shimming a High-Resolution MAS Probe

A. Sodickson\* and D. G. Cory†<sup>1</sup>

\*Harvard/MIT Division of Health Sciences and Technology and †Department of Nuclear Engineering,  
Massachusetts Institute of Technology, NW14-4111, 150 Albany Street,  
Cambridge, Massachusetts 02139

Received January 14, 1997

**A systematic and efficient approach to shimming a high-resolution, magic angle sample spinning probe is introduced. The method takes into account the different symmetries of the normal shim coils and the MAS experiment.** © 1997 Academic Press

Magic angle sample spinning (MAS) is developing as a powerful tool for the study of semisolids, including the important examples of combinatorial chemistry (1) and excised tissues (2). These recent applications have been facilitated by the development of high-resolution MAS probes where care is taken to use susceptibility matched materials and MAS gradient probes (3) which permit excellent water suppression and gradient selection of coherence pathways. Here, a systematic approach to shimming these high-resolution probes is discussed, which takes into account the different symmetries of the normal shim coils and the MAS experiment.

Since the NMR resonance frequency is directly proportional to the magnetic field strength, the NMR lineshape reflects the variation of the magnetic field strength over the sample volume. This rather obvious conclusion has led to the requirement that any high-resolution NMR experiment be preceded by a tedious period of shimming, and a culture has been established around this art, along with a hierarchy of methods aimed at obtaining the best field homogeneity. An abundance of manual, computer-assisted, and gradient-based mapping methods is established for the high-resolution liquid state experiment that may provide excellent resolution for the initiate (useful general references are (4, 5)).

The case of shimming an MAS probe is distinct from the liquid state geometry, both because of the high rates of sample spinning involved and because the spinning axis does not lie along the field direction. Very early, Bloch (6)

pointed out that mechanical motion can be used to coherently average selected spatial variations of the magnetic field. A coherent modulation of an inhomogeneous interaction will subdivide the spectrum into a sharpened central band and a collection of sidebands. The intensity of these sidebands varies as Bessel functions whose arguments are proportional to the residual off-axis inhomogeneity divided by the spinning speed. If the modulation frequency is on the order of the field inhomogeneity then the sidebands have an observable intensity. Hence shim sets include two categories of correction coils, the zonal shims which are cylindrically symmetric about the sample axis and are thus not averaged by the spinning, and the tesseral shims which possess lesser symmetry, whose task it is to reduce the off-axis field variations sufficiently that sidebands are not troublesome. With the importance today of multidimensional experiments, and a desire to avoid  $t_1$  noise (7), it has become routine to study stationary samples, and the zonal and tesseral shims may be weighted more equally.

In MAS experiments, the spinning is employed for coherent averaging of contributions to the NMR linewidth from susceptibility variations (8) and residual dipolar couplings (9). The spinning rates are typically at least a few kilohertz, much faster than the inhomogeneous linewidth due to spatial variations in the field. In this case, the amplitudes of the sidebands are always small, and shimming may be focused on that set of shims that have cylindrical symmetry about the MAS spinner axis. The most natural approach to shimming for high-resolution MAS probes is thus to use a set of zonal shims whose symmetry axis is oriented along the spinner axis.

Detailed descriptions of typical shim coils have been presented elsewhere (4, 10). They are designed to produce  $z$  components of the magnetic field whose magnitudes vary as spherical harmonics. The shims may be described in the laboratory frame as being composed of zonal harmonics—those that have cylindrical symmetry about  $z$ —and tesseral

<sup>1</sup> To whom correspondence should be addressed. Fax: (617) 253-5405. E-mail: dcory@mit.edu.

TABLE 1

## Laboratory Frame Zonal Shims in Cartesian Coordinates

$$\begin{aligned}
B_z^0 &= T_0 = 1 \\
B_z^1 &= T_1 = z \\
B_z^2 &= 2T_2 = 2z^2 - (x^2 + y^2) \\
B_z^3 &= 2T_3 = 2z^3 - 3z(x^2 + y^2) \\
B_z^4 &= 8T_4 = 8z^4 - 24z^2(x^2 + y^2) + 3(x^2 + y^2)^2 \\
B_z^5 &= 48T_5 = 6[8z^5 - 40z^3(x^2 + y^2) + 15z(x^2 + y^2)^2]
\end{aligned}$$

harmonics, which vary azimuthally about the sample. They are presented in Cartesian coordinates in Tables 1 and 2, and are proportional to the surface spherical harmonic basis functions

$$\begin{aligned}
T_n &= r^n P_n(\cos \theta), \\
T_{nm}^{(e)} &= r^n P_{nm}(\cos \theta) \begin{pmatrix} \cos m\phi \\ \sin m\phi \end{pmatrix}, \quad [1]
\end{aligned}$$

where  $P_n$  and  $P_{nm}$  are, respectively, the Legendre polynomials and the associated Legendre polynomials. Note that the angular dependence of the even and odd tesseral basis func-

TABLE 2

## Laboratory Frame Tesseral Shims in Cartesian Coordinates

$$\begin{aligned}
&\text{First order} \\
B_x &= T_{11}^e = x \\
B_y &= T_{11}^o = y \\
&\text{Second order} \\
B_{zx} &= \frac{1}{3} T_{21}^e = zx \\
B_{zy} &= \frac{1}{3} T_{21}^o = zy \\
B_{x^2-y^2} &= \frac{1}{3} T_{22}^e = (x^2 - y^2) \\
B_{xy} &= \frac{1}{6} T_{22}^o = xy \\
&\text{Third order} \\
B_{z^2x} &= \frac{2}{3} T_{31}^e = x(4z^2 - (x^2 + y^2)) \\
B_{z^2y} &= \frac{2}{3} T_{31}^o = y(4z^2 - (x^2 + y^2)) \\
B_{z(x^2-y^2)} &= \frac{1}{15} T_{32}^e = z(x^2 - y^2) \\
B_{xyz} &= \frac{1}{30} T_{32}^o = xyz \\
B_x^3 &= \frac{1}{15} T_{33}^e = x^3 - 3xy^2 \\
B_y^3 &= \frac{1}{15} T_{33}^o = 3yx^2 - y^3
\end{aligned}$$

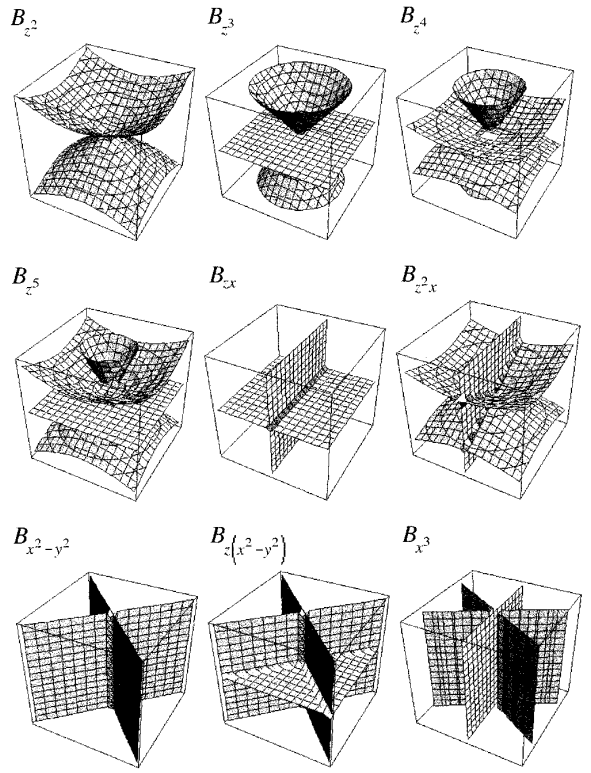


FIG. 1. Isometric plots of the nodal surfaces for selected shims. The fields shown correspond, from left to right, to the zonal shims  $z^2$ ,  $z^3$ ,  $z^4$ , and  $z^5$  and the even-symmetry tesseral shims  $zx$ ,  $z^2x$ ,  $(x^2 - y^2)$ ,  $z(x^2 - y^2)$ , and  $x^3$ . Note in particular that the nodal surface for the  $z^2$  shim includes the magic angle. The odd-symmetry tesseral shims may be visualized simply by rotating the plots for the corresponding even-symmetry shims by  $\pi/2m$ , where  $m = 1$  for  $zy$  and  $z^2y$ ,  $m = 2$  for  $xy$  and  $xyz$ , and  $m = 3$  for  $y^3$ .

tions comprises linear combinations of the standard  $Y_{n,\pm m}$  spherical harmonics whose azimuthal dependence is instead  $e^{\pm im\phi}$ .  $T_n$  and  $T_{nm}$  form a complete orthonormal basis set. They are truly orthogonal only over a spherical volume, however, resulting in the unfortunate interactions between shims that are observed when the shim fields are integrated over cylindrical sample geometries. Correction fields of higher order  $n$  are required to eliminate field inhomogeneities that vary as higher orders of any given spatial coordinate.

The shims presented in Tables 1 and 2 cover the 18 nominal shims found in wide-bore systems and in older standard bore shim sets. As shown in the tables, the zonal shims are complete through fifth order, while the tesseral shims are only complete through third order. The reasons are twofold; the number of tesseral shims grows as twice the order, and the shim sets are optimized for correcting field variations along the long axis of the sample. A complete set of shims through fifth order numbers 36 and the extra shims add greatly to the complexity of the shim set and to the overall currents used for correcting the field. Figure 1 shows a col-

lage of selected shims demonstrating the underlying symmetries of the shims and their increasing complexity as a function of order. The displayed surfaces are the nodal planes of the correction fields.

The desired set of zonal shims along the MAS axis could, of course, be implemented by a new set of gradient windings, but there is no need since through third order a complete set of spherical harmonic fields exists. Since the laboratory frame correction fields form a complete set of basis functions, any desired field profile up to third order may be expressed as a linear combination of the laboratory frame shims. For ease of shimming under MAS conditions, it is only necessary to transform the existing shims into a set that is oriented along the MAS spinner axis, and then to explore the extent of averaging introduced by MAS. To third order the shim set is complete, and may thus be transformed into a set at any orientation. The transformation from the laboratory frame into the MAS axis system depends on their azimuthal relationship, so for the results that follow the  $z$  axis of this tilted frame has been arbitrarily chosen to be aligned at  $[\sqrt{2}/3, 0, \sqrt{1}/3]$  relative to the laboratory frame. In other words, the MAS spinner axis is assumed to be aligned with the  $x$  axis of the laboratory frame shim set.

For this spinner orientation, the tilted MAS reference frame and the laboratory frame share a common  $y$  axis, and a rotation about this axis through  $-\theta_m$  transforms the MAS coordinates to laboratory frame coordinates. Any physical rotation of a spherical harmonic results in a linear combination of harmonics of the same order but all  $m$  values. In addition, the transformed  $T_{nm}$  state will include contributions only from states that share the same even or odd azimuthal symmetry:

$$\begin{aligned} T_{nm}^e(r, \theta, \phi) &= \sum_{m'=0}^n c_{m'} T_{nm'}^e(r', \theta', \phi'), \\ T_{nm}^o(r, \theta, \phi) &= \sum_{m'=1}^n c_{m'} T_{nm'}^o(r', \theta', \phi'). \end{aligned} \quad [2]$$

Furthermore, from the addition formula of spherical harmonics it is straightforward to derive the transformations for the zonal shims,

$$\begin{aligned} T_n(r, \theta, \phi) &= \sum_{m=0}^n \epsilon_m \frac{(n-m)!}{(n+m)!} P_{nm}(\cos \theta_m) T_{nm}(r', \theta', \phi'), \end{aligned} \quad [3]$$

where  $\epsilon_m = 2 - \delta_{m,0}$ , and the unprimed MAS frame transforms to the primed laboratory frame simply by a rotation through  $-\theta_m$  about their shared  $y$  axes. The tesseral shims may be transformed using the Wigner rotation matrix elements  $D_{m,m'}(0, -\theta_m, 0)$ . Alternatively, the coordinate trans-

**TABLE 3**  
**Spherical Harmonic Shims in the Tilted Frame Expressed as Linear Combinations of Laboratory Frame Shims**

---

First order	
$B_z^{\text{tilt}} = \frac{1}{\sqrt{3}} B_z^{\text{lab}} - \frac{\sqrt{2}}{\sqrt{3}} B_x^{\text{lab}}$	
$B_x^{\text{tilt}} = \frac{1}{\sqrt{3}} B_x^{\text{lab}} + \frac{\sqrt{2}}{\sqrt{3}} B_z^{\text{lab}}$	
$B_y^{\text{tilt}} = B_y^{\text{lab}}$	
Second order	
$B_{z^2}^{\text{tilt}} = B_{(x^2-y^2)}^{\text{lab}} - 2\sqrt{2} B_{zx}^{\text{lab}}$	
$B_{zx}^{\text{tilt}} = -\frac{1}{3} B_{zx}^{\text{lab}} + \frac{\sqrt{2}}{6} B_{z^2}^{\text{lab}} - \frac{\sqrt{2}}{6} B_{(x^2-y^2)}^{\text{lab}}$	
$B_{zy}^{\text{tilt}} = \frac{1}{\sqrt{3}} B_{zy}^{\text{lab}} - \frac{\sqrt{2}}{\sqrt{3}} B_{xy}^{\text{lab}}$	
$B_{(x^2-y^2)}^{\text{tilt}} = \frac{2\sqrt{2}}{3} B_{zx}^{\text{lab}} + \frac{1}{3} B_{z^2}^{\text{lab}} + \frac{2}{3} B_{(x^2-y^2)}^{\text{lab}}$	
$B_{xy}^{\text{tilt}} = \frac{1}{\sqrt{3}} B_{xy}^{\text{lab}} + \frac{\sqrt{2}}{\sqrt{3}} B_{zy}^{\text{lab}}$	
Third order	
$B_{z^3}^{\text{tilt}} = -\frac{2}{3\sqrt{3}} B_{z^3}^{\text{lab}} - \frac{1}{\sqrt{6}} B_{z^2x}^{\text{lab}} + \frac{5}{\sqrt{3}} B_{z(x^2-y^2)}^{\text{lab}} - \frac{5}{3\sqrt{6}} B_{x^3}^{\text{lab}}$	
$B_{z^2x}^{\text{tilt}} = \frac{\sqrt{2}}{3\sqrt{3}} B_{z^3}^{\text{lab}} - \frac{\sqrt{3}}{2} B_{z^2x}^{\text{lab}} + \frac{5}{6\sqrt{3}} B_{x^3}^{\text{lab}}$	
$B_{z^2y}^{\text{tilt}} = -\frac{10\sqrt{2}}{3} B_{xyz}^{\text{lab}} + \frac{1}{6} B_{z^2y}^{\text{lab}} + \frac{5}{6} B_{y^3}^{\text{lab}}$	
$B_{z(x^2-y^2)}^{\text{tilt}} = \frac{1}{3\sqrt{3}} B_{z^3}^{\text{lab}} - \frac{\sqrt{2}}{3\sqrt{3}} B_{x^3}^{\text{lab}}$	
$B_{xyz}^{\text{tilt}} = -\frac{1}{3} B_{xyz}^{\text{lab}} + \frac{\sqrt{2}}{12} B_{z^2y}^{\text{lab}} - \frac{\sqrt{2}}{12} B_{y^3}^{\text{lab}}$	
$B_{x^3}^{\text{tilt}} = \frac{\sqrt{2}}{3\sqrt{3}} B_{z^3}^{\text{lab}} + \frac{1}{2\sqrt{3}} B_{z^2x}^{\text{lab}} + \frac{2\sqrt{2}}{\sqrt{3}} B_{z(x^2-y^2)}^{\text{lab}} + \frac{5}{6\sqrt{3}} B_{x^3}^{\text{lab}}$	
$B_{y^3}^{\text{tilt}} = 2\sqrt{2} B_{xyz}^{\text{lab}} + \frac{1}{2} B_{z^2y}^{\text{lab}} + \frac{1}{2} B_{y^3}^{\text{lab}}$	
Fourth order	
$B_{z^4}^{\text{tilt}} = -\frac{7}{18} B_{z^4}^{\text{lab}} + \sum_{m=1}^4 c_m T_{4m}$	
Fifth order	
$B_{z^5}^{\text{tilt}} = -\frac{1}{6\sqrt{3}} B_{z^5}^{\text{lab}} + \sum_{m=1}^5 c_m T_{5m}$	

---

formations may of course be performed in Cartesian coordinates, and the results decomposed into the laboratory frame shim fields of the same order and symmetry as the original tilted frame shim.

Table 3 presents the spherical harmonic shims in the magic-angle-tilted reference frame, expressed in terms of the normal laboratory frame shims. Again, note that these are

complete to third order, but there is no possible transformation for the fourth- and fifth-order zonal spins, *vide infra*. So under nonspinning conditions with the sample tilted at the magic angle, the field may be shimmed to third order in exactly the manner accustomed from high-resolution work, provided that the appropriate subset of shims is varied in concert. The fourth- and fifth-order laboratory frame shims, if varied, will contribute to the desired zonal shims in the tilted frame, although they will of course also transform into other harmonic fields of the same order and even azimuthal symmetry.

Under spinning conditions, only the zonal shims in the tilted frame will contribute and hence shimming becomes simpler. As discussed above, spinning sidebands are negligible since the spinning rate is much greater than the line broadening due to field inhomogeneities. The only surviving shims are thus the zonal shims  $B_{z^1}^{\text{tilt}}$  through  $B_{z^5}^{\text{tilt}}$  in the spinning frame, which, being invariant to rotation about the spinner axis, still transform to the same linear combination of laboratory frame shims listed in Table 3. As none of the odd-symmetry shims contribute to the zonal harmonics in the tilted frame,  $B_y^{\text{lab}}$ ,  $B_{zy}^{\text{lab}}$ ,  $B_{xy}^{\text{lab}}$ ,  $B_{z^2y}^{\text{lab}}$ ,  $B_{xyz}^{\text{lab}}$ , and  $B_{y^3}^{\text{lab}}$  are all averaged completely by spinning, and current to these shims may thus be eliminated when spinning. In fact, spinning quickly about any axis in the  $x$ - $z$  plane would eliminate contributions from these laboratory frame shims, as the  $x$ - $z$  plane is one of the nodal planes for each of these shims. In addition, the  $B_{z^2}^{\text{lab}}$  shim has absolutely no influence on the NMR lineshape under MAS, due to the specific choice of the magic angle for the spinning axis. As seen in Fig. 1, this shim contains a nodal plane exactly along the magic angle—the field varies as the second Legendre polynomial  $P_2(\cos \theta) = 1/2(3 \cos^2 \theta - 1)$ , which of course disappears at the magic angle  $\theta_m = \cos^{-1}(1/\sqrt{3})$ .

Of particular interest are the fourth- and fifth-order shims, for which the laboratory frame tesseral components were not implemented, so the only possibility is to employ the residual variation of these zonal shims. These laboratory frame shims transform into the MAS frame zonal shims, which survive spinning, and into MAS frame tesseral shims of the same order, which are eliminated by spinning. From Eq. [3],  $B_{z^4}^{\text{lab}}$  and  $B_{z^5}^{\text{lab}}$  transform into  $B_{z^4}^{\text{tilt}}$  and  $B_{z^5}^{\text{tilt}}$  with efficiencies of  $-7/18$  and  $-1/6\sqrt{3}$ , respectively. The absence of the other fourth- and fifth-order laboratory frame shims simply reduces the efficiency with which the MAS frame correction fields may be produced. Nonetheless, MAS frame zonal shims through fifth order are all created perfectly when spinning, as spinning itself serves to eliminate all but the zonal contributions.

This observation in fact leads to a simplified approach to shimming when spinning. While varying the shim fields in concert according to the linear combinations of Table 3 will

produce the proper correction field geometries even when the sample is stationary, alternatively, when spinning, one need only choose a single laboratory frame shim to substitute for the appropriate MAS frame  $n$ th-order zonal shim  $B_{z^n}^{\text{tilt}}$ . Choosing the terms that contribute with the highest efficiency in the linear combinations of Table 3 (and including the weighting factors from Table 2), this suggests the use of  $B_x^{\text{lab}}$ ,  $B_{zx}^{\text{lab}}$ ,  $B_{z^2x}^{\text{lab}}$ ,  $B_{z^4}^{\text{lab}}$ , and  $B_{z^5}^{\text{lab}}$  as the surrogate  $n$ th-order shims. If these coils cannot produce strong enough fields for adequate shimming, current may be applied to the other shims in the linear combination, with the appropriate sign. Of course, these choices and the weighting factors in Table 3 rely on the weighting factors listed in Tables 1 and 2 connecting the shims to their corresponding spatial harmonics. The exact weightings will in fact be shim-set dependent, varying with the coil geometry used and the number of windings. To shim a spinning sample, these efficiencies are not crucial, and trial and error will quickly determine which of the laboratory frame coils in the linear combination contributes most efficiently in practice to the MAS frame zonal correction field. If one were to attempt to shim in the tilted frame while stationary, however, the actual efficiencies become more important, as inappropriate shim combinations will produce not only the desired zonal shims but also other tesseral shims of the same order.

It should further be realized that the results of Table 3 and the conclusions drawn above all rely on the fact that the spinner is oriented in the  $x$ - $z$  plane. This relative orientation may be tested in practice by observing that the  $y$  shim or any other odd-symmetry shim has no influence on the NMR lineshape in an MAS experiment. If the azimuthal alignment of the spinner and shim set is off by a phase angle  $\psi$ , then the laboratory frame shims must be transformed further by a rotation about the  $z$  axis. The even- and odd-symmetry tesseral shims of a given  $m$  value will transform cyclically into one another as  $m\psi$  under this rotation:

$$T_{nm}^{(\circ)} \rightarrow T_{nm}^{(\circ)} \cos(m\psi) \pm T_{nm}^{(\circ)} \sin(m\psi). \quad [4]$$

This effect must of course be taken into account either to align the spinner in the laboratory frame  $x$ - $z$  axis or to modify the linear combinations of Table 3 to include laboratory frame shims of the other symmetry as well.

In summary, some appreciation for the geometries and symmetries of typical correction fields leads to a simple and useful approach to high-resolution shimming under MAS. To shim a tilted but stationary sample, correction fields of the proper geometry in the tilted frame can be produced by varying the currents through the laboratory frame shims in the proper ratios, which requires knowledge of the coil efficiencies in the actual shim set. Spinning, however, eliminates all but those correction field components that are cylindri-

cally symmetric about the spinner axis, greatly simplifying the task at hand. Current may be removed entirely from the laboratory frame shims that do not contribute to the MAS frame zonal shims— $B_{z^2}^{\text{lab}}$  and those with odd symmetry when the spinner is aligned in the  $x$ - $z$  plane. Any laboratory frame shim that contributes to the linear combinations of the transformed zonal shims in Table 3 then contributes only a correction field of the same order that is cylindrically symmetric in the MAS frame. One or more of the contributing shims may be used in any ratio in place of a true  $B_{z^2}^{\text{tilt}}$  shim coil.

### ACKNOWLEDGMENTS

Insightful discussions with Dr. Martine Ziliox and Dr. Werner Maas are gratefully acknowledged, as is support from the Department of Energy and the National Institute for Health (R01-GM52026-01, RR-0095).

### REFERENCES

1. R. C. Anderson, M. A. Jarema, M. J. Shapiro, J. P. Stokes, and M. Ziliox, *J. Org. Chem.* **60**, 2650 (1995).
2. L. L. Cheng, C. L. Lean, A. Bogdanova, S. C. Wright, J. L. Ackerman, T. J. Brady, and L. Garrido, *Magn. Reson. Med.* **36**, 653 (1996).
3. W. E. Maas, F. H. Laukien, and D. G. Cory, *J. Am. Chem. Soc.* **118**, 13085 (1996).
4. C. N. Chen and D. I. Hoult, "Biomedical Magnetic Resonance Technology," Chap. 3, Adam Hilger, Bristol, 1989.
5. V. W. Miner and W. W. Conover, "Shimming Ain't Magic," Acorn NMR, Fremont, CA (1992).
6. F. Bloch, *Phys. Rev.* **94**, 496 (1954).
7. A. F. Mehlkopf, D. Korbee, T. A. Tiggelman, and R. Freeman, *J. Magn. Reson.* **58**, 315 (1984).
8. A. N. Garroway, *J. Magn. Reson.* **49**, 168 (1982).
9. E. R. Andrew and R. G. Eades, *Nature* **183**, 1802 (1959).
10. F. Roméo and D. I. Hoult, *Magn. Reson. Med.* **1**, 44 (1984).